

Electronic Supplementary Information (ESI)

A Room Temperature Solid State Dual-Ion Battery Based on Gel Electrolyte

Shuai Wang,^{a,#} Xiang Xiao,^{a,#} Chaopeng Fu,^c Jiguo Tu,^a Yuanyuan Tan,^a and Shuqiang Jiao^{*,a,b}

^a*State Key Laboratory of Advanced Metallurgy, University of Science and Technology Beijing, Beijing, 100083, P. R. China. *E-mail: sjiao@ustb.edu.cn*

^b*Beijing Key Laboratory for Magneto-Photoelectrical Composite and Interface Science, University of Science and Technology Beijing, 100083, P. R. China*

^c*School of Materials Science and Engineering, Shanghai Jiao Tong University, Shanghai 200240, P. R. China*

[#]*These authors contributed equally to this work.*

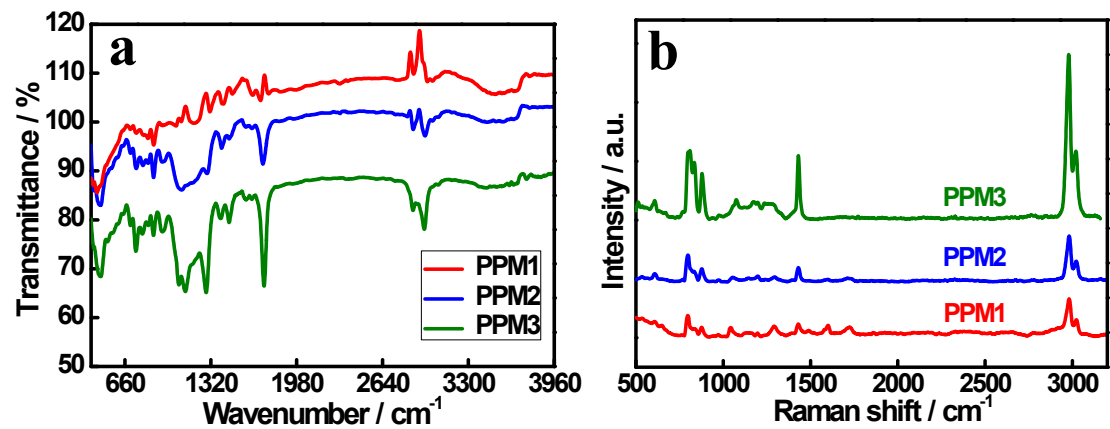


Fig. S1 (a) FTIR spectra of PPM1, PPM2, and PPM3. (b) Raman spectra of PPMs.

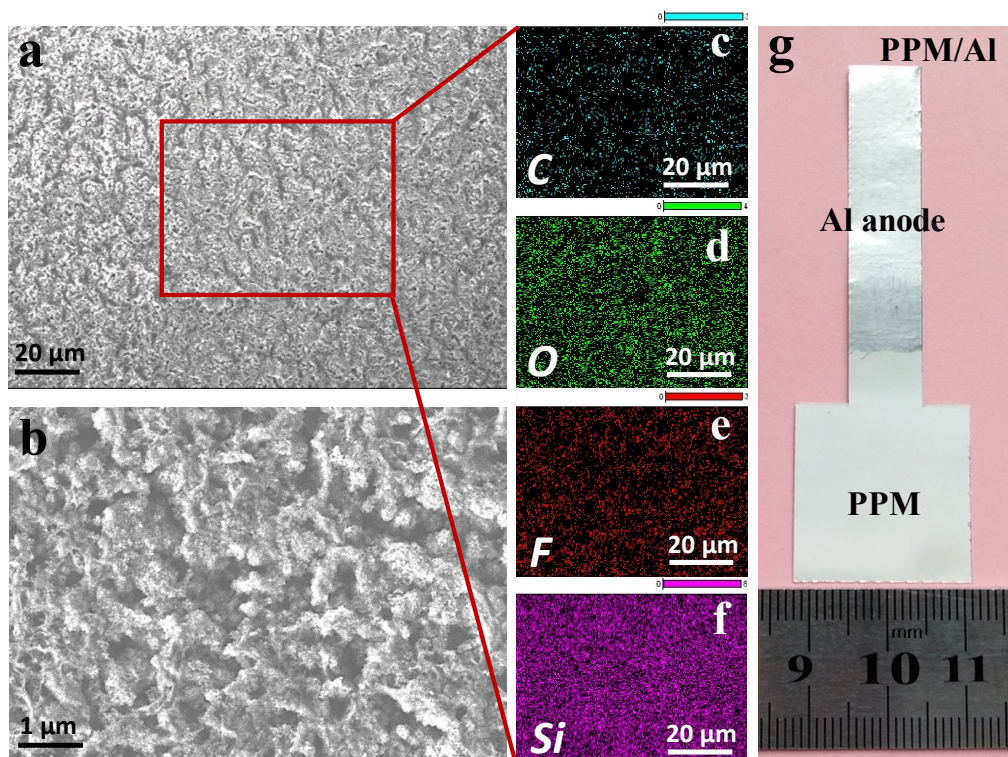


Fig. S2 (a) FE-SEM images of the micro-porous membranes. (b) The magnified view of (a). (c-f) The corresponding EDX spectra of black boxed area in (a). (g) The digital photo of PPM/Al.

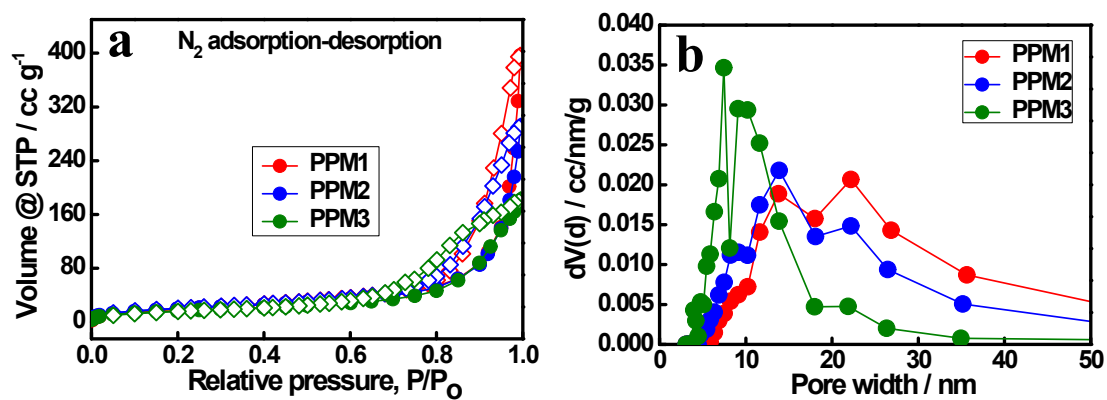


Fig. S3 (a) N₂ adsorption-desorption isotherm plots (77.3 K on carbon) for PPMs. (b) The mesopore size distributions of PPMs for N₂, calculated by using the Barrett-Joyner-Halenda (BJH) method.

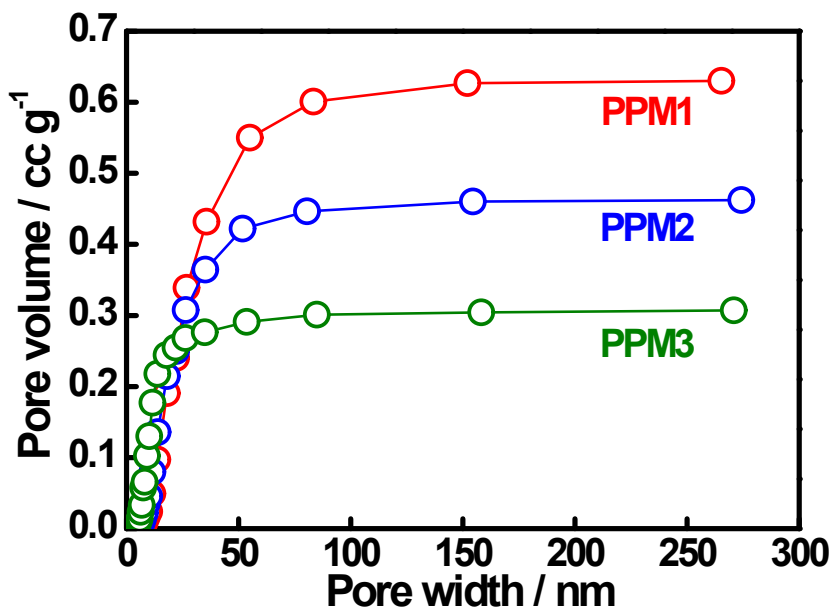
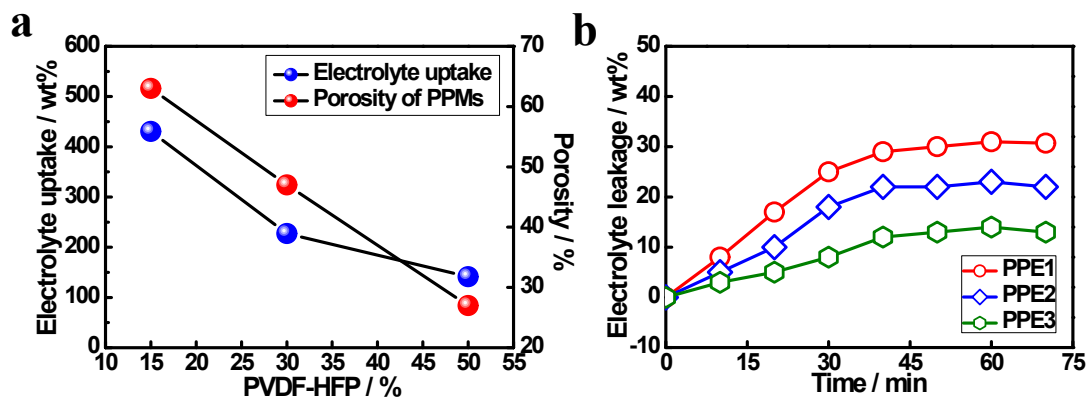


Fig. S4 Total mesopore volumes of PPM1, PPM2, and PPM3. Actual Fitting Error <1.000%.



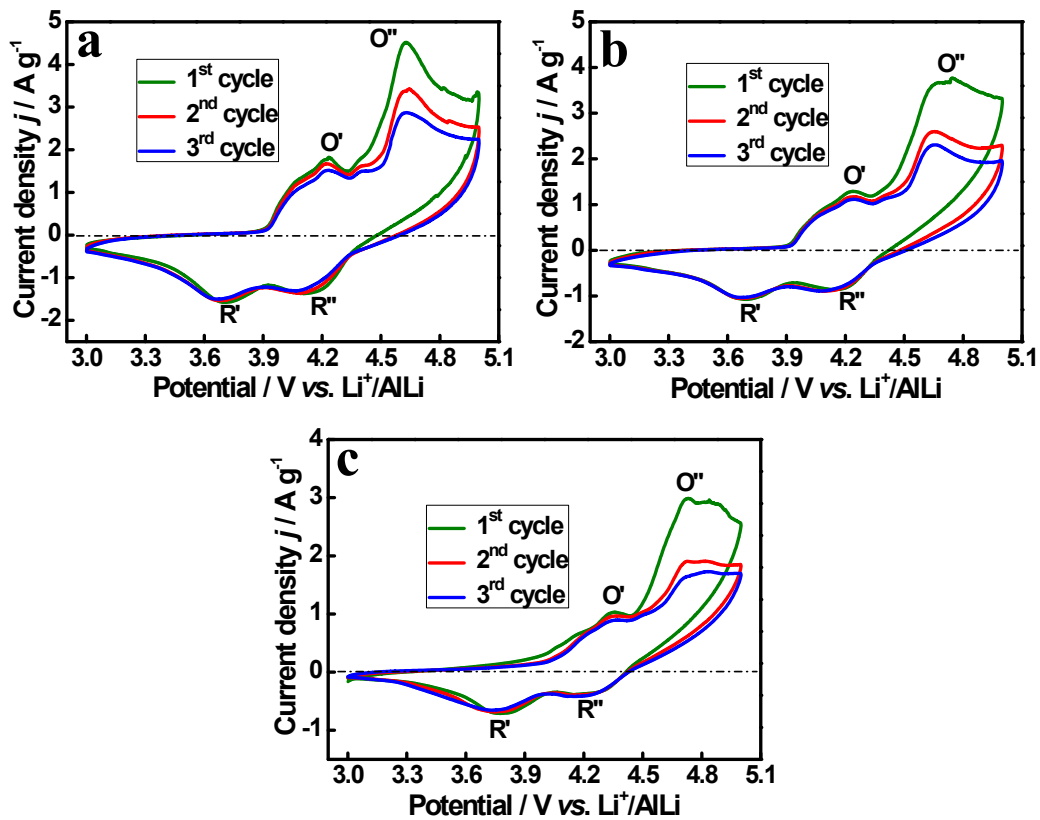
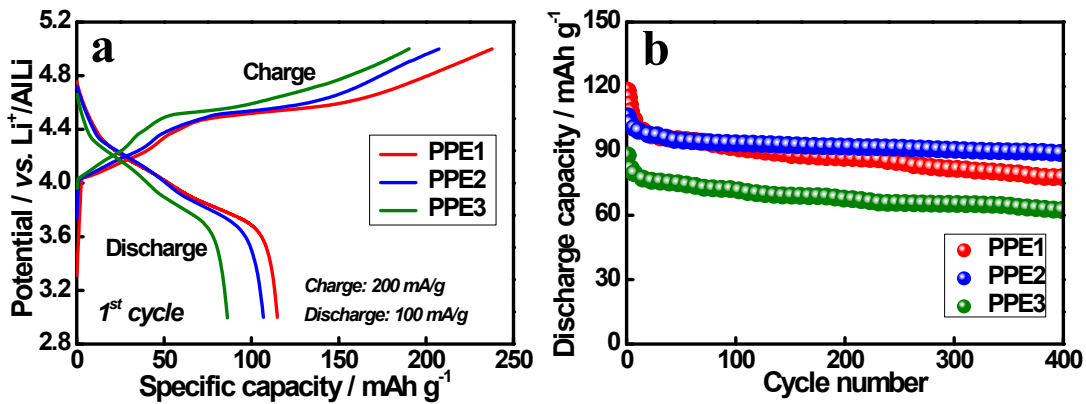


Fig. S6 CV curves of the dual-ion batteries with different PPEs at 5.0 mV s^{-1} over the range of 3.0~5.0 V. (a) PPE1, (b) PPE2, and (c) PPE3.



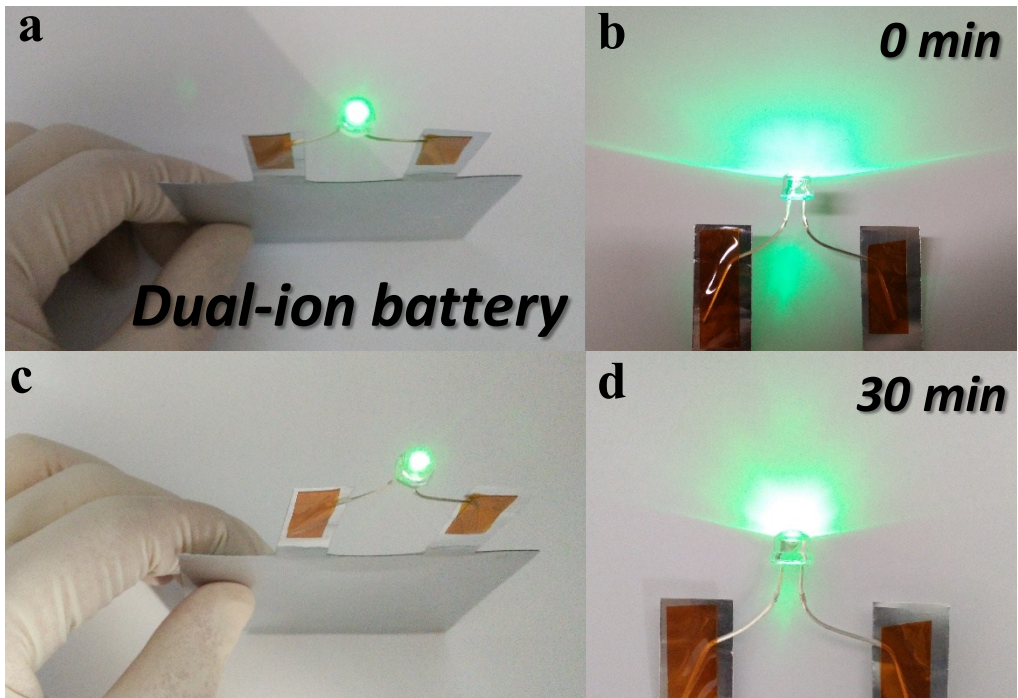


Fig. S8 The solid state dual-ion battery demonstration. (a,b) A picture showing that a cell can light up a green LED lamp, powered by the fully charged cell. (c,d) Images of the green LED lamp after lighting 30 mins.

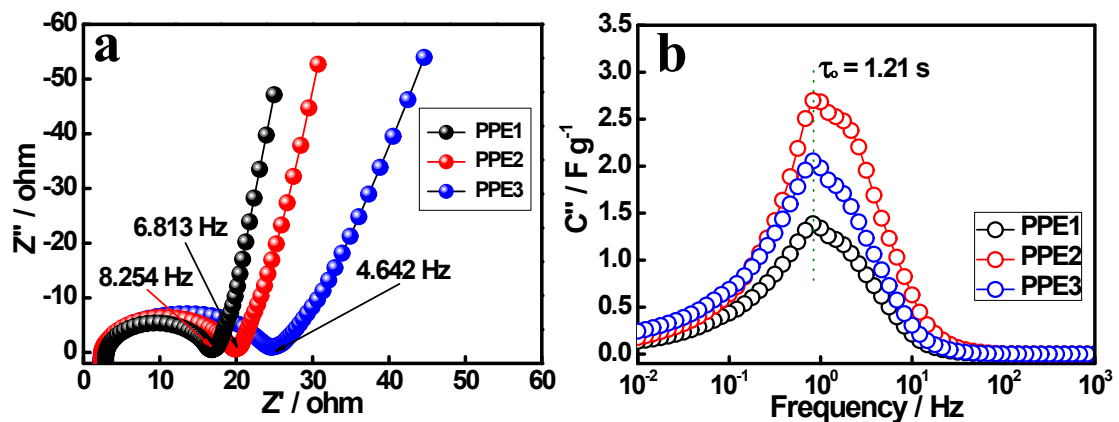


Fig. S9 (a) Nyquist plots of the dual-ion batteries with different PPEs obtained by electrochemical impedance spectroscopy (EIS) tests under the open circuit potential (4.0 V). (b) Plots of the imaginary capacitance *versus* the frequency.

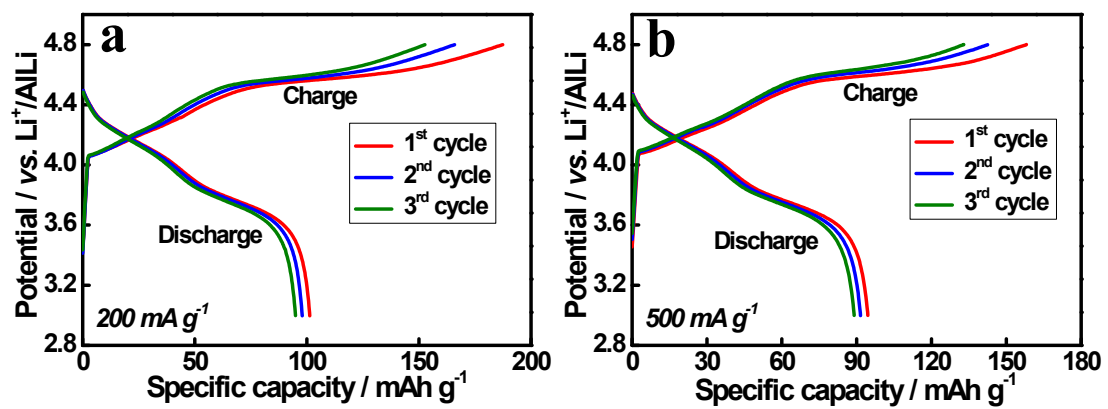


Fig. S10 The initial three charge/discharge curves of the dual-ion batteries with PPE2 at the same charge and discharge current densities. (a) 200 mA g⁻¹, and (b) 500 mA g⁻¹.

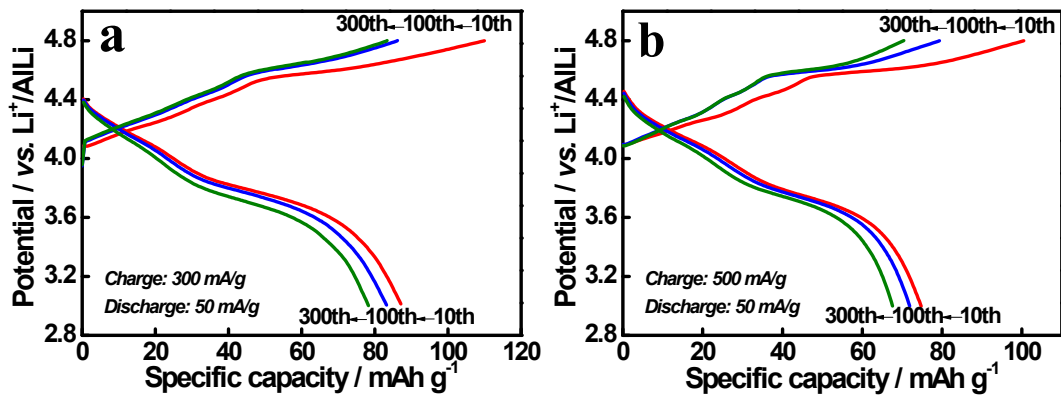


Fig. S11 The typical charge/discharge curves during various cycles at the higher charge current

densities. (a) Charge current density: 300 mA g^{-1} , and (b) Charge current density: 500 mA g^{-1} .

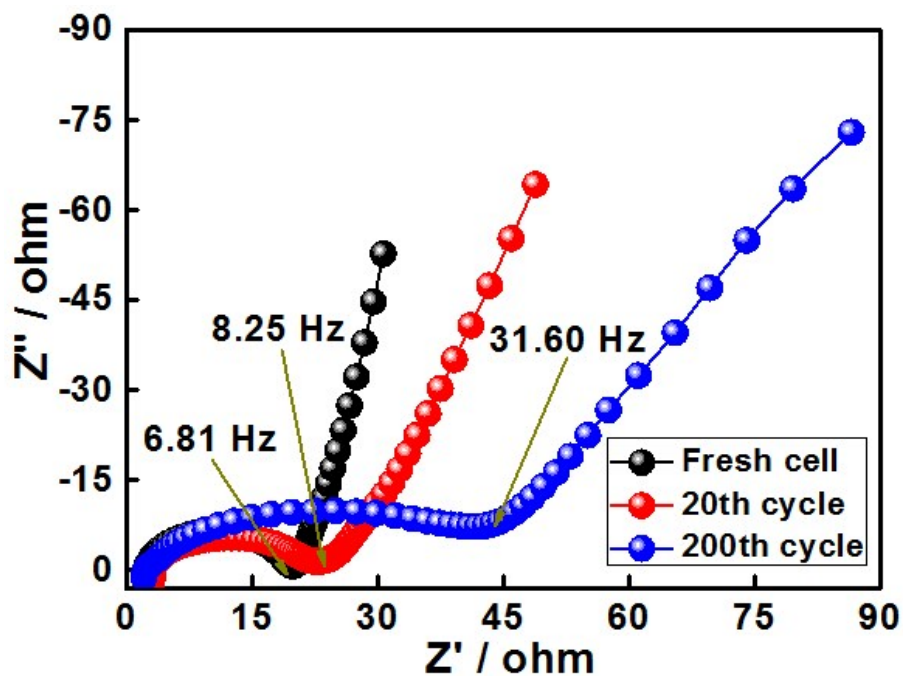


Fig. S12 Nyquist plots for the dual-ion battery with PPE2 after 0, 20, and 200 cycles.

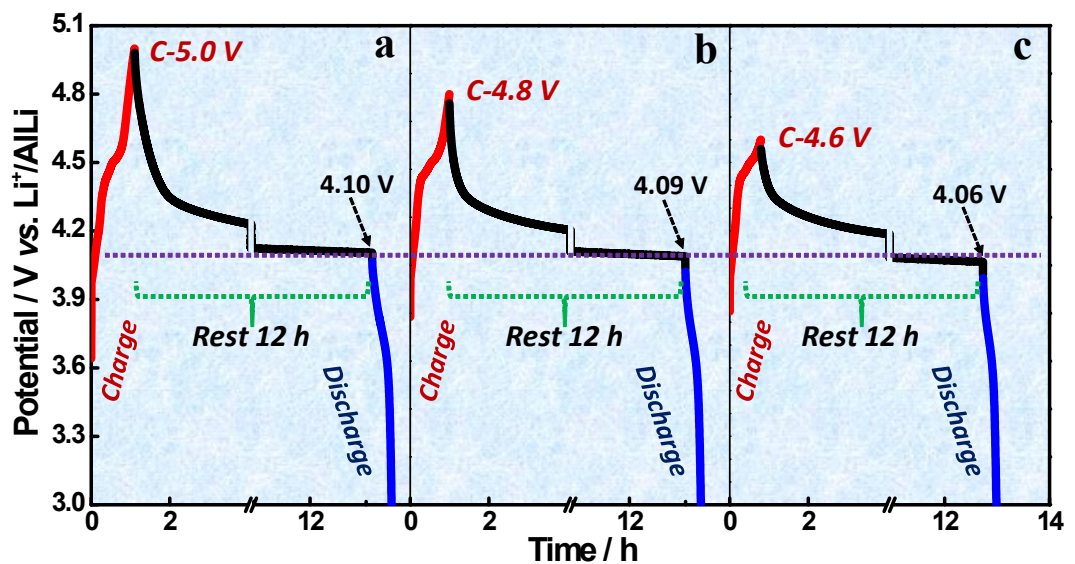


Fig. S13 Self-discharge behaviors of the dual-ion battery under different charge cut-off voltages. The rest time: 12 hrs.

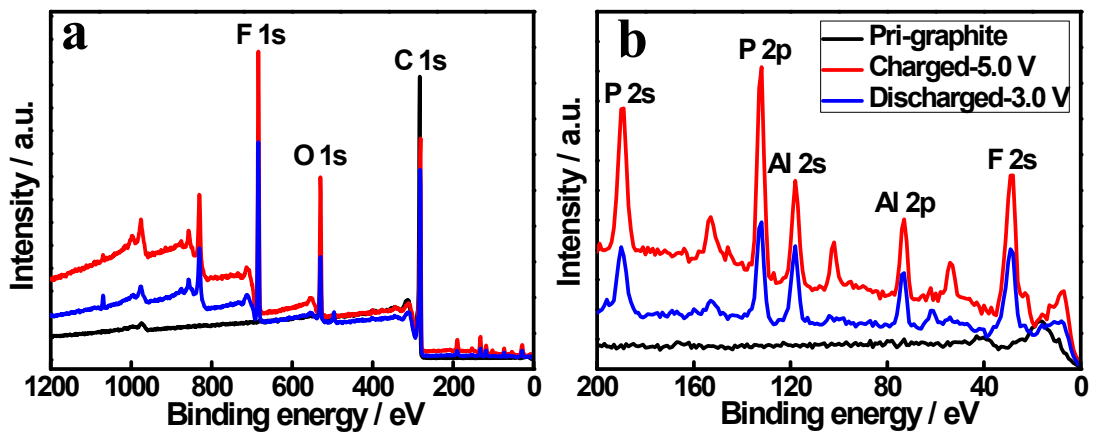


Fig. S14 (a) Wide survey XPS spectra of the graphite cathodes at different states. (b) Close-up view of (a) from 0~200 eV.

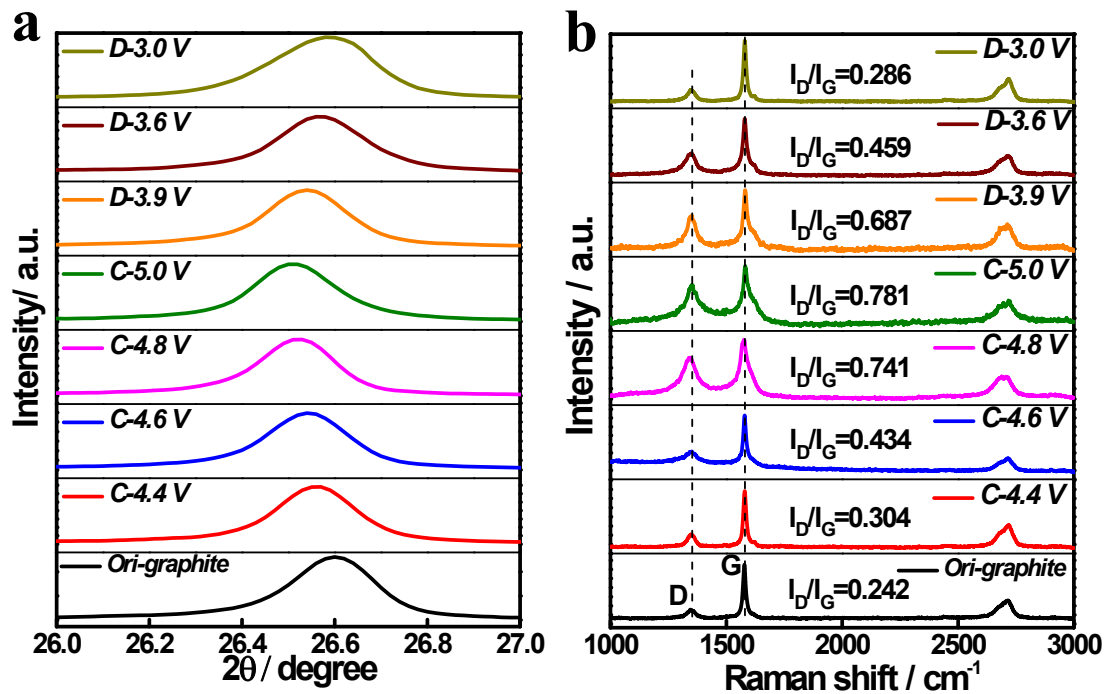


Fig. S15 *Ex-situ* characterizations of the cathodes in various charging and discharging voltage.

(a) *Ex-situ* XRD patterns. (b) *Ex-situ* Raman spectra.

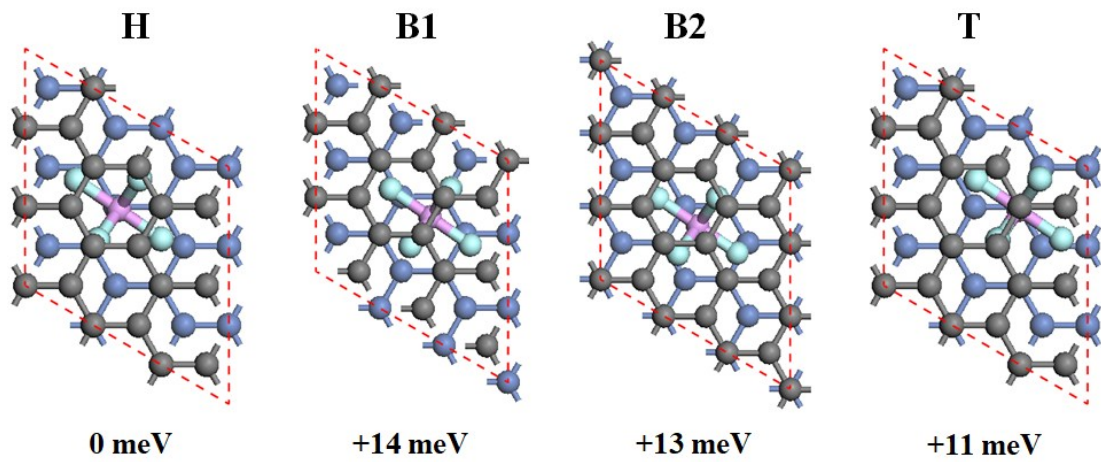


Fig. S16 Four possible configurations of PF_6^- intercalation in graphite bilayer. Energies relative to the most stable geometry (H) were shown with each structure. The pink and cyan balls indicated phosphorus and fluorine atom, respectively. For better contrast, two graphite layers (upper and lower) were denoted by grey and light blue balls, respectively.

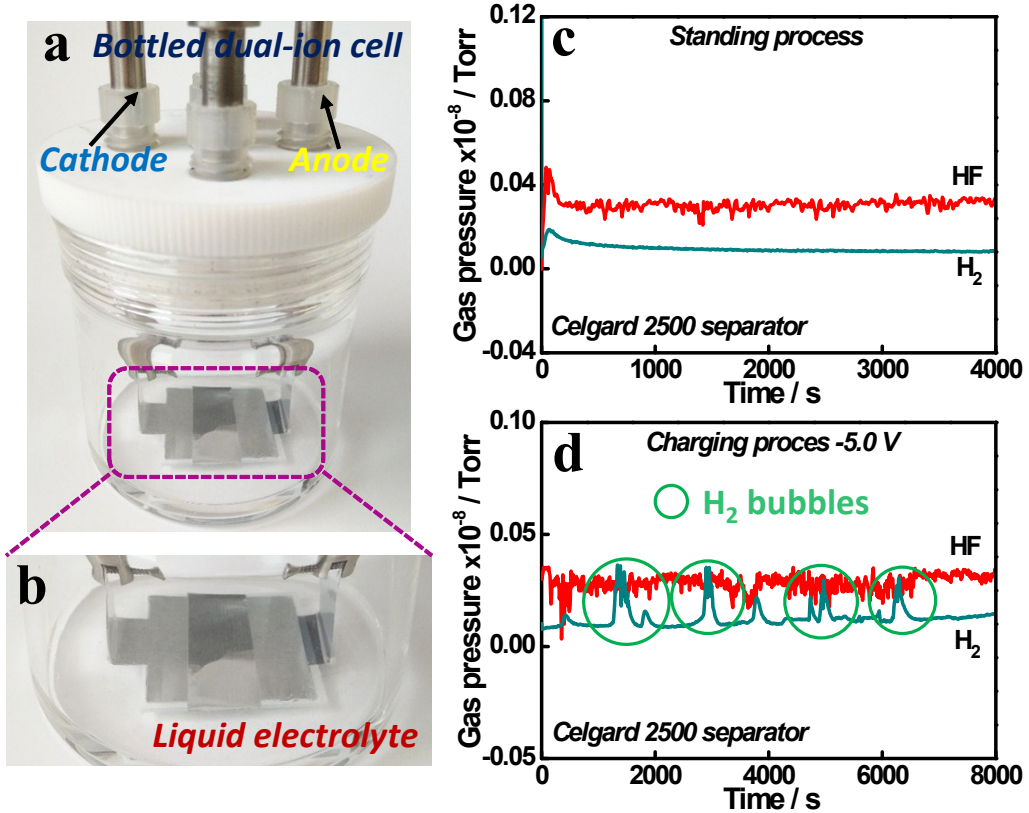


Fig. S17 Gas behavior with the liquid electrolyte. (a) The bottled dual-ion battery with 2500 separator. (b) The partial enlargement of (a). (c) The *in-situ* gas partial pressure of the dual-ion battery with the liquid electrolyte during standing process. (d) The same battery system as (c) during charging process (Charged-5.0 V).

Table S1 EDX analyses results of the micro-porous polymer membranes.

Samples		C-K	O-K	F-K	Si-K
<i>PPM1</i>	<i>wt%</i>	14.04	28.97	26.51	30.48
	<i>at%</i>	21.43	33.19	25.49	19.89
<i>PPM2</i>	<i>wt%</i>	10.62	28.23	32.70	28.45
	<i>at%</i>	16.42	32.76	31.96	18.86
<i>PPM3</i>	<i>wt%</i>	11.67	26.35	39.47	22.51
	<i>at%</i>	17.67	29.96	37.79	14.58

Table S2 Textural characteristics of the micro-porous membranes.

Samples	BET surface area (m ² /g)	Total pore volume* (cc/g)	Mesopore volume (cc/g)	Mesopore width (nm)
PPM1	74.76	0.647	0.630	22.180
PPM2	72.68	0.475	0.463	13.880
PPM3	60.14	0.355	0.307	7.463

* Pore with dimensions up to 999 Å by NLDFT, assuming carbon slit pore geometry.

Table S3 EIS analyses results of the batteries based on the different micro-porous gel electrolytes.

Samples	R _s (Ω)	R _{ct} (Ω)	CPE _{1-T} (×10 ⁻⁵)	CPE _{1-P}	R _p (Ω)	W _{o-R}	W _{o-T}	W _{o-P}
PPM1	3.15	16.29	2.18	0.93	13.03	4.05	0.98	0.44
PPM2	2.40	19.44	3.16	0.88	16.95	3.32	0.61	0.43
PPM3	2.32	23.64	6.52	0.80	21.51	6.96	1.07	0.39

Table S4 EIS analyses results of the battery based on the micro-porous gel electrolyte (PPE2)

at the zeroth, 20th, and 200th cycle, respectively.

Samples	R _s (Ω)	R _{ct} (Ω)	CPE _{1-T} T(×10 ⁻⁵)	CPE _{1-P}	R _p (Ω)	W _{o-R}	W _{o-T}	W _{o-P}
<i>Fresh cell</i>	2.40	19.44	3.16	0.88	16.95	3.32	0.61	0.43
<i>20th cycle</i>	3.32	22.27	8.41	0.78	19.31	11.42	1.49	0.37
<i>200th cycle</i>	2.63	38.27	7.41	0.85	39.42	19.40	6.05	0.68

Table S5 Net charge of PF_6^- calculated by Mulliken method.^[8]

System	P	F	Total
PF_6^-	2.87	-0.48	-0.01
<i>PF_6^- intercalated in graphite bilayer</i>	2.8	-0.62	-0.92